atoms

MDPI

*Article*

# TDCS Calculation for the Ionization of Nitrogen Molecule by Electron Impact

**Alpana Pandey and Ghanshyam Purohit ***

Department of Physics, University College of Science, Mohanlal Sukhadia University, Udaipur 313001, India; alpana0129@gmail.com
* Correspondence: ghanshyam.purohit@mlsu.ac.in

**Abstract:** Triple differential cross section (TDCS) results are reported for the electron impact ionization of nitrogen molecules. The TDCSs have been calculated in distorted wave Born formalism using orientation averaged molecular orbital (OAMO) approximation. The TDCS results are presented as average and weighted sum for the outer molecular orbital $3\sigma_g$, $1\pi_u$, $2\sigma_u$ and the inner $2\sigma_g$ molecular orbital. The obtained theoretical TDCSs are compared with the available measurements. The results are analysed in terms of the positions and relative intensities of binary and recoil peaks. Within a first order model and for a complex molecule, a reasonable agreement is obtained with the experimental data in the binary peak region with certain discrepancies in position and magnitude in the recoil peak region.

**Keywords:** TDCS; weighted and average sum; DWBA; PCI; correlation polarization



**Citation:** Pandey, A.; Purohit, G. TDCS Calculation for the Ionization of Nitrogen Molecule by Electron Impact. *Atoms* **2022**, *10*, 50. https://doi.org/10.3390/atoms10020050

Academic Editor: Jean-Christophe Pain and Himadri Chakraborty

Received: 18 April 2022
Accepted: 14 May 2022
Published: 18 May 2022



## 1. Introduction

Over the past three decades, electron impact ionization studies have gained considerable experimental and theoretical attention. Atomic and molecular physicists consider electron impact ionization of targets such as atoms, ions and molecules to be one of the most important collision processes. Electron impact ionization also referred to as (e, 2e) [1] involves the collision of a projectile (incident electron) with a target (either an atom or an ion or a molecule) leading to the ionization of the target. Upon determining the energies and the momenta of all the particles involved in the collision, one can have a complete understanding of the ionization process. Thus, (e, 2e) collisions have become an important tool for investigating the collision dynamics of targets. The triple differential cross section (TDCS) is the physical quantity that is of prime interest in these studies, it provides information about collision processes, ionization mechanisms, and the dependence of the ionization process on the electron kinematics under which ionization is taking place. Experimental techniques such as cold target recoil-ion momentum spectroscopy (COLTRIM) [2] and recoil-ion spectroscopy (RMS) [3] have been instrumental to obtain the cross-sections of the electron impact ionization of atomic and molecular targets.

Most of the experimental efforts have been focused on inert gas atoms [4], and limited attempts have been made to measure cross-sections of molecular targets and the theoretical support also has been less for these measurements. It is mainly due to the experimental difficulties in measuring TDCS for molecules, as a result of the close spacing of the different molecular states, and the difficulty of developing a theoretical model to explain molecular ionization, as a consequence of the multi-centre nature of the target. There have been efforts to study the electron impact ionization of molecular targets [5–8]. The TDCS has been calculated for various molecular targets, from simple diatomic atoms to very complex molecules. Some of these studies may be mentioned; $H_2$ [9–11], $N_2$ [12–17], $CO_2$ [18], $H_2O$ [19–21] and a wide range of biologically complex molecules like pyrimidine [22], thymine [23] etc. Electron impact single ionization cross-sections of molecular targets can be calculated by using various theoretical techniques. One of the most successful theoretical

models to study electron impact ionization of various targets is the distorted-wave Born approximation (DWBA) [24]. The single ionization of a complex target can be viewed as a three-body problem in which the spectator electrons are represented by spherically symmetric potentials. In the DWBA formalism, these spherically symmetric potentials can be utilized in Schrödinger equation to calculate the continuum wave functions. In the Born approximation, it is not possible to obtain exact solutions to the Schrödinger equation. Therefore, it is impossible to describe all the interactions and processes that may take place during ionization. It is possible to modify the theoretical formalism in several ways, such as by approximating the post-collision interaction (PCI), taking into account correlation-polarization effects, and considering the electron exchange.

In the low to intermediate impact energy region, diatomic molecules $H_2$ and $N_2$ and the triatomic $H_2O$ and $CO_2$ are ionized as given in most of the recent studies. Several studies [25–27] have been done for $N_2$, where TDCS is calculated at different projectile energy. The electron impact cross sections of $N_2$ molecules have been calculated using the distorted wave Born approximation (DWBA) method [28]. DWBA has been found to give a reasonable agreement with the measurements for the (e, 2e) studies on molecules with certain discrepancies, particularly in the recoil peak region.

In the present communication, we investigate the ionization of nitrogen molecules at different energies within the distorted-wave Born approximation formalism using the orientation-averaged molecular orbital approximation. We report the TDCS results for the ionization of nitrogen molecules at scattered electron energy 500 eV, for the coplanar asymmetric emission of electrons [29]. In the present study, we have used atomic units ($\hbar$ = e = $m_e$ = 1) for all calculations. In the next section, we outline the theoretical approach used to calculate TDCS.

## 2. Theory

The initial—state Hamiltonian chosen in the standard DWBA is given by

$$H_0 = H_{target} + T_p + U_i \tag{1}$$

where $H_{target}$ is the Hamiltonian for the neutral target, $T_p$ is the kinetic energy operator for the projectile and $U_i$ is an initial-state spherically symmetric potential for the ionization process. The DWBA approach was generalized to molecules [30,31].

The triple differential cross section for the ionization of nitrogen molecule by electron impact is given by

$$\frac{d^3\sigma}{dk_s dk_e dE_e} = (2\pi)^4 \frac{k_s k_e}{k_i} |t|^2, \tag{2}$$

where $k_s$, $k_e$, $k_i$ are the momenta of the scattered, ejected and the incident electrons, respectively. The term $E_e$ and 't' is referred to as ejected electron energy and transition matrix element respectively. The transition matrix is represented in the terms of direct and exchange scattering amplitude. The amplitude is given by

$$|t|^2 = |f_{dir}|^2 + |f_{ex}|^2 - |f_{dir}||f_{ex}| \tag{3}$$

where the direct scattering amplitude $(f_{dir})$ is given by

$$f_{dir} = < X_s(r_1)X_e(r_2)|\frac{(-Z)}{r_{12}}|X_b(r_2)X_i(r_1) > \tag{4}$$

Similarly, the exchange term $(f_{ex})$ can be expressed as

$$f_{ex} = < X_e(r_1)X_f(r_2)|\frac{(-Z)}{r_{12}}|X_b(r_2)X_i(r_1) > \tag{5}$$

In this equation, $r_1$, $r_2$ are the position vectors for projectile and active electron, and $r_{12}$ is the distance between projectile and active target electron. For incident, bound, and

scattered electrons, $X_i$, $X_b$, $X_s$ represent their distorted wave functions, respectively. The bound state for the orbitals of the $N_2$ molecule is approximated as the orientation averaged molecular orbital where. The molecular wave function has been calculated using the B3LYP/TZ2P [32] basis sets based on density functional theory. We calculate the distorted waves on symmetric potential, which is based on the Hartree-Fock charge distribution for $N_2$ averaged over all molecular orientations. For the incoming electron wave function, the Schrödinger equation is given by

$$(T + U_i - \frac{k_i^2}{2})x_i(k_i, r) = 0 \tag{6}$$

T represents the kinetic energy operator. In the initial state, the distortion potential is determined by the nuclear contribution and the electronic contribution i.e.,

$$U_{static} = U_{el} + U_{nuc} \tag{7}$$

By averaging the two $N_2$ nuclei over all orientations, we get the nuclear part. It is obtained as a result of placing the nuclear charge on a spherical shell with a radius equal to the distance of the nucleus from the centre of mass. From the calculated molecular charge density averaging over all angular orientations, the electronic part is derived. The final state distorted potential is generated in a similar way except that the active electron is removed from the charge distribution. The distorting potential proposed by Furness and McCarthy [33], which was later corrected by Riley and Truhlar [34] is added to the static Hartree—Fock distorting potential. The exchange—distortion potential $U_E$ generated for same is given by

$$U_E = 0.5[E_0 - U_{static}(r) - (E_0 - U_{static}(r))^2 + 4\pi\rho(r)] \tag{8}$$

To calculate the TDCSs, we have also included the correlation polarization potential $U_{CP}$ in the distorting potential which is given by

$$U_{CP} = U_{SR}^{Corr}(r), r \leq r_0 \tag{9}$$

$$= \frac{-\alpha_d}{2r^4}, r > r_0 \tag{10}$$

$U_{SR}^{Corr}(r)$ is the short range correlation potential [35] and $\alpha_d$ dipole polarizability of the target.

We have treated the post collision interaction between the two outgoing particles by the Ward-Macek approximation [36]. In the ward-Mack approximation, one replaces the actual final state e-e separation $r_{12}$ by an average value directed parallel to $k_{12}$. The average separation is given by

$$r_{12}^{ave} = \frac{\pi^2}{16}(1 + \frac{0.627}{\pi}\sqrt{\epsilon}ln\epsilon)^2 \tag{11}$$

$\epsilon$ is the total energy of the two exiting electrons. With this approximation, the ward-Macek factor is given by

$$M_{ee} = \frac{\gamma}{\exp(\gamma) - 1}|_1F_1(i\lambda, 1, -2ik_{12}r_{12}^{ave}) \tag{12}$$

Where, $\frac{\gamma}{\exp(\gamma)-1} = N_{ee}$ ,which is the Gamow factor.

Also, $\gamma = \frac{-2\pi}{k_1-k_2}$ , $\lambda = \frac{1}{k_1-k_2}$

The present model DWBA is employed to calculate the TDCS for the ionization of the outer $3\sigma_g$, $1\pi_u$, $2\sigma_u$ and the 'inner' $2\sigma_g$ molecular orbital of the nitrogen molecule by electron impact. The results and discussion is presented in the next section.

## 3. Results and Discussion

In the present study, we report the results of TDCS calculated in the distorted wave Born approximation approach for the electron impact single ionization of nitrogen molecules which includes orientation-averaged molecular orbital approximation. We have calculated TDCSs for the ionization of nitrogen molecules from 'outer' valence orbital $3\sigma_g$, $1\pi_u$, $2\sigma_u$ and the 'inner' $2\sigma_g$ molecular orbital, these orbital have 15.6, 16.7, 18.75 and 39.9 eV ionization potentials respectively. As the electronic states of the three outer orbital are very closely spaced, it is difficult to be resolved. Therefore, the weighted sum of TDCS for $3\sigma_g$, $1\pi_u$, $2\sigma_u$ orbital with relative efficiencies of 1, 0.78, and 0.32 have also been plotted.

The angular distribution of TDCSs are reported for scattered electron energy $E_s$ = 500 eV and scattering angle $-6^0$ at ejected electron energies $E_e$ = 37 eV, $E_e$ = 74 eV and $E_e$ = 205 eV and the obtained results are compared with the available measurements [29]. The experimental TDCSs [29] and TDCSs obtained by present study are analyzed in terms of the magnitude of binary and recoil peak and their respective positions. Along with the peak positions and intensity, the recoil-to-binary peak ratios have been obtained and compared for measurements [29] as well as for the theoretically obtained results. The TDCSs have been computed in standard DWBA formalism with first Born term. TDCS calculations are also reported including the correlation-polarization potential and PCI effects in the standard DWBA.

The present results are plotted in Figures 1–3 for ejected electron energies $E_e$ = 37 eV, $E_e$ = 74 eV and $E_e$ = 205 eV. The solid red circles are the experimental TDCS [29]. The solid curve is for DWBA results with first Born term calculated for the average sum of the orbitals. The dashed curve is DWBA results including correlation polarization potential, and the dotted curve represents DWBA calculations including polarization potential and PCI effects. The dark circles, upside triangles and hollow circles represent the standard DWBA results, DWBA with polarization potential and DWBA with polarization potential and PCI with the weighted sum of the orbital respectively.

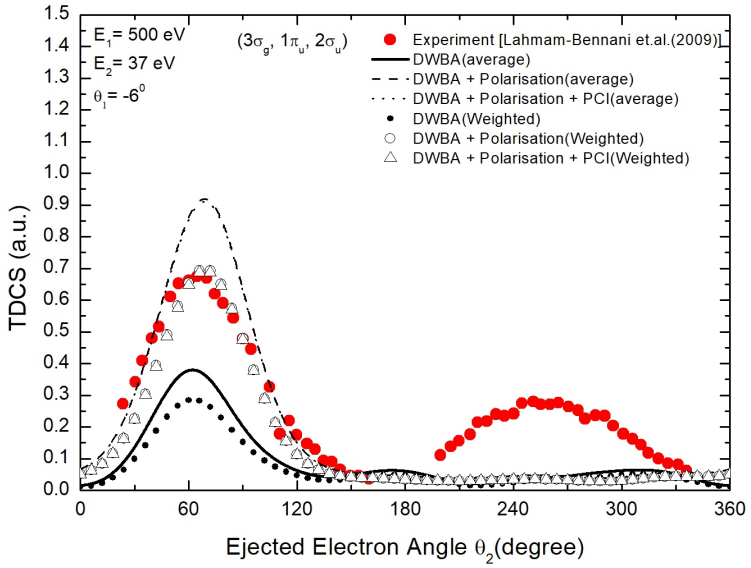


**Figure 1.** Electron-impact TDCS for $N_2$ molecule calculated for the weighted and average sum of the outer orbital ($3\sigma_g$, $1\pi_u$, $2\sigma_u$). The ejected electron energy is 37 eV. Kinematics and legends used are displayed in the figure frame.

The TDCS results are presented for ejected electron energy 37 eV in Figure 1. A good agreement with experimental results [29] has been obtained in the present standard DWBA with first Born term as well as the DWBA results including correlation-polarization potential and PCI in the binary peak region, particularly in terms of the binary peak positions. The DWBA results calculated by including polarization potential and PCI with weighted sum

of orbital are in very good agreement with the measurements [29] in terms of binary peak positions as well as magnitude of the binary lobe. In the binary peak region, the standard DWBA results for average and weighted sum shows the binary peaks at ejected electron angle 61° and 62° in comparison to the experimental binary peak obtained at 65°. The binary peaks of the TDCS curve calculated using DWBA including polarization and PCI for both average and weighted sum are shifted towards higher ejected electron angles at 69°. It is observed that the experimental TDCS shows recoil peak in the range of 200°–300° with the recoil peak position around 260° . Theoretical TDCS fails to reproduce the recoil peak in the same range and the magnitude of theoretical recoil peak also does not match with the experimental data.

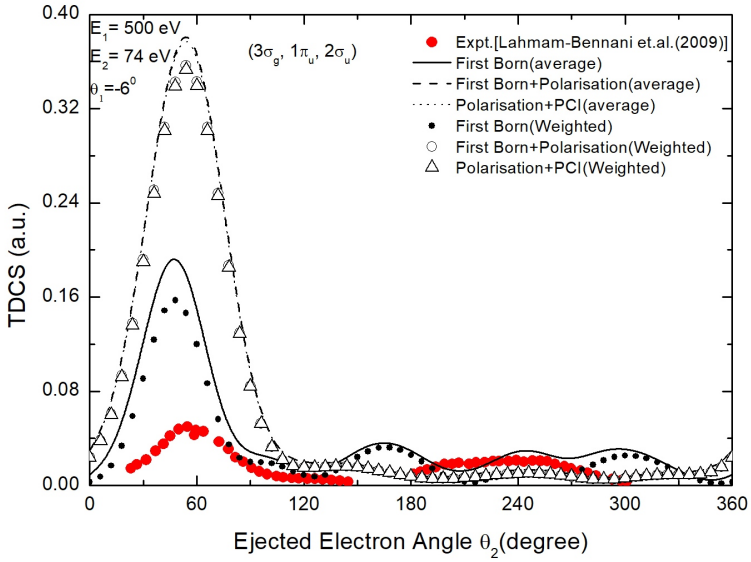


**Figure 2.** Same as Figure 1. The ejected electron energy is 74 eV.

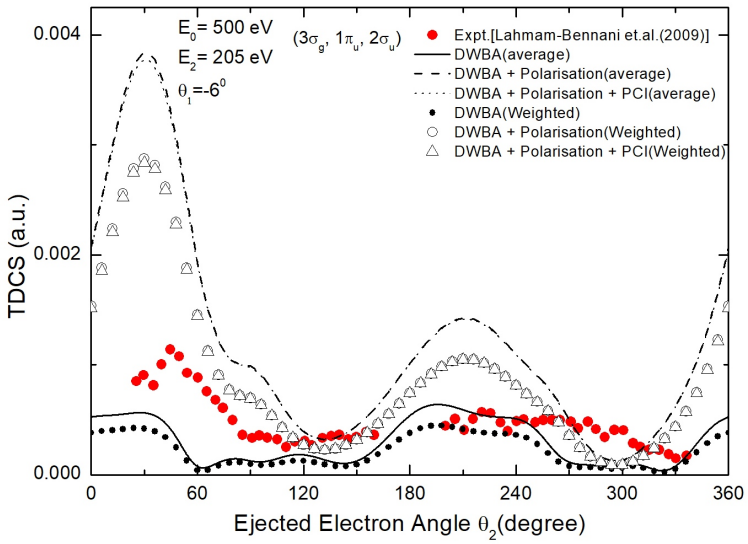


**Figure 3.** Same as Figure 1. The ejected electron energy is 205 eV.

As shown in Figure 2, the calculated and experimental TDCSs are for an ejected electron energy of 74 eV. Both the weighted and average sums of the binary peak's position show discrepancies in the binary region, and there is less agreement with the experimental data for smaller ejection angles compared with higher ejection angles. It is observed that polarization potential and PCI are not very significant at this ejected electron energy. In terms of binary peak, the theoretical peaks obtained are shifted towards lower ejection

angles relative to the experimental binary peak. The recoil to binary peak ratio obtained in the present theoretical TDCS results does not match with the experimental data [29]. The theoretical results with weighted sum including polarization and PCI show a smaller recoil peak, however the standard DWBA results show more than a two-peak structure.

At ejected electron energy $E_e$ = 205 eV, the binary peaks observed in the theoretical TDCSs are shifted towards the lower ejection angle in comparison to the measurements [29]. Both the weighted sum of the orbitals and the average sum of the orbitals fails to reproduce the position of the experimental binary peak and there is also disagreement in the recoil to binary peak ratio. In case of Recoil peak, the theoretical models present better results, however there are discrepancies in the position of the recoil peak. Despite the fact that there are no experimental points for ejection angles smaller than 20°, the measured data show some sign of a binary peak splitting.

Along with weighted and average sum of the outer orbitals, we have analysed TDCS results in terms of $3\sigma_g$, $1\pi_u$, $2\sigma_u$ contribution individually. In Figure 4, the TDCS results are presented for the ejection energy 37 eV. It can be observed that the TDCS corresponding to the $1\pi_u$, including polarization potential is the major contributor to the weighted and average sum of the orbitals in the binary region. There is large discrepancy in the trends of TDCS in the recoil peak region. There is a huge discrepancy in the recoil to binary peak ratio.

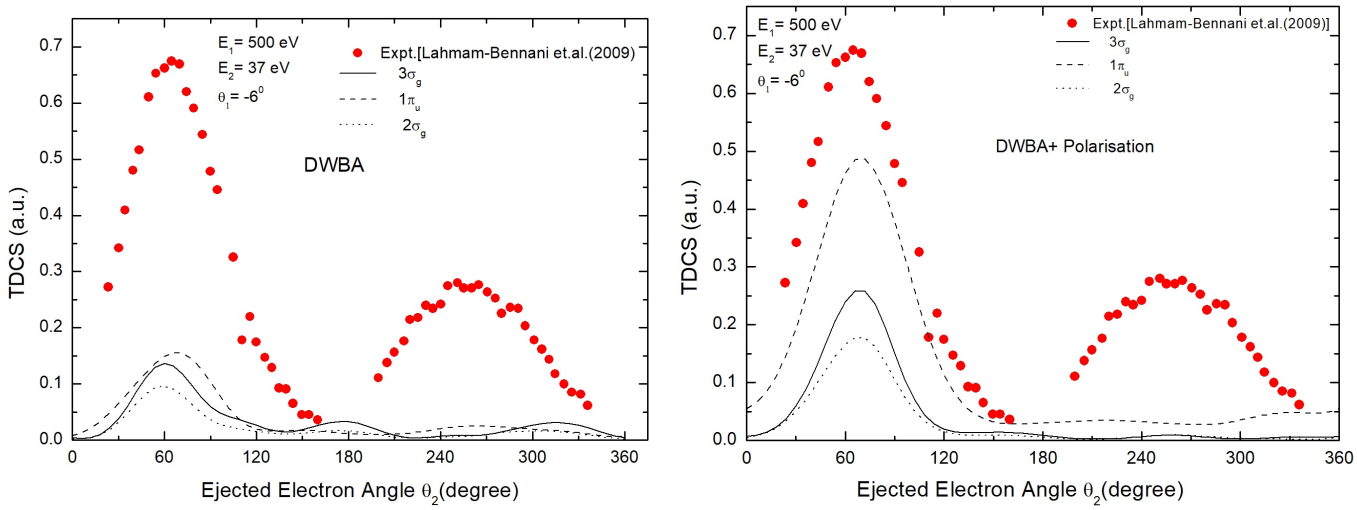


**Figure 4.** Electron-impact TDCS for $N_2$ molecule calculated for $3\sigma_g$, $1\pi_u$, $2\sigma_u$ valence orbitals. The ejected electron energy is 37 eV. (**a**) Individual orbital contribution for TDCS calculated by DWBA formalism, (**b**) shows contribution of individual orbital calculated by including polarisation potential. Kinematics and legends used are displayed in the figure frame.

We can see a totally different situation in Figure 5, where we analyse orbitals at ejection energy 74 eV. The size of the contribution of $1\pi_u$, $2\sigma_u$ is nearly equal to the experimental TDCS. Furthermore, it may be observed that the recoil to binary ratio of these orbitals is nearly the same. However, $3\sigma_g$ show different behaviour and fails to reproduce the experimental results.

In Figure 6, the TDCS obtained by DWBA and correlation polarisation potential at ejected energy 205 eV is presented. In both the cases, highest contribution is given by $1\pi_u$, which also gives a higher recoil to binary peak ratio in the case of DWBA, including polarization potential results compared to the $2\sigma_u$ , $3\sigma_g$ orbitals, while the recoil peak is small for the DWBA formalism. We can also see a significant difference between these formalisms at the binary peak.

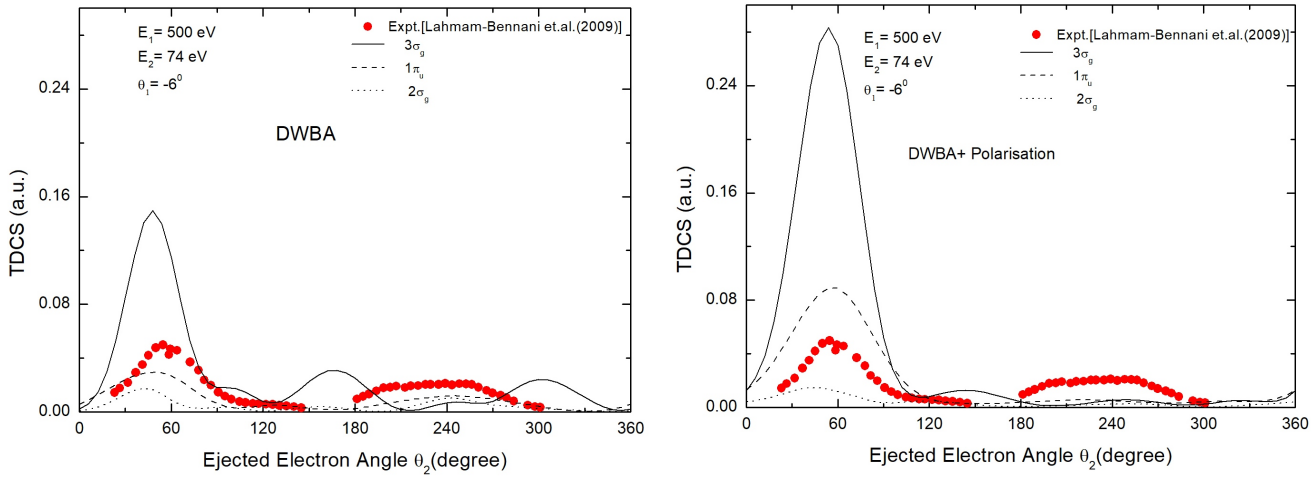


**Figure 5.** Same as Figure 4 at ejected electron energy 74 eV.

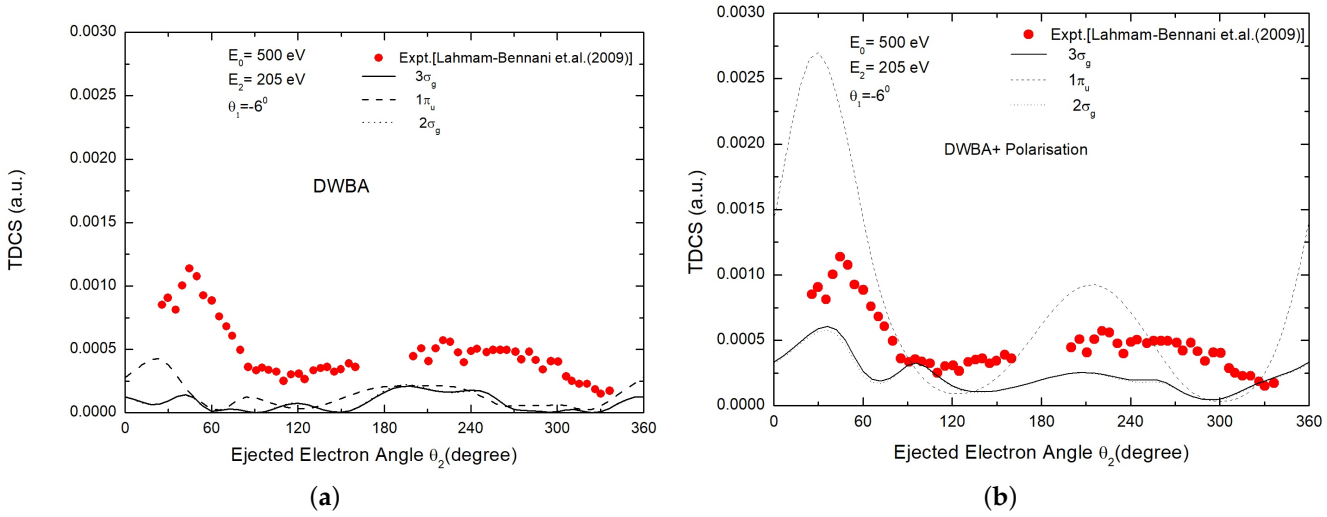


**Figure 6.** Same as Figure 4 at ejected electron energy 205 eV.

Besides, calculating TDCS corresponding to the ionization of nitrogen molecules from the outer orbital, we have also calculated TDCSs for the ionization from inner orbital. TDCSs obtained for the ionization taking place from $2\sigma_g$ orbitals at 36 eV, 74 eV, and 205 eV ejected energies are presented in Figures 7–9. It can be seen that the theoretical models give fair agreement with the experimental data in the binary region. However, significant differences are observed between the theoretical and experimental results in the recoil region. There is no prominent difference between the theoretical TDCS obtained by correlation potential and PCI effect. On the other hand, it appears that experimental binary peak for the inner orbitals in the binary peak region is well reproduced by the TDCS including polarization potential.

TDCSs obtained for 37 eV ejection energy are plotted in Figure 7. The TDCS obtained by including polarization potential shows reasonable agreement with the binary peak of measurements [29] however fails to reproduce the recoil peak as observed in measurements. The theoretical TDCS including polarization potential shows different behaviour for inner and outer orbitals. In case of inner orbitals the TDCS calculated by including polarization potential are in better agreement with the measurements [29].

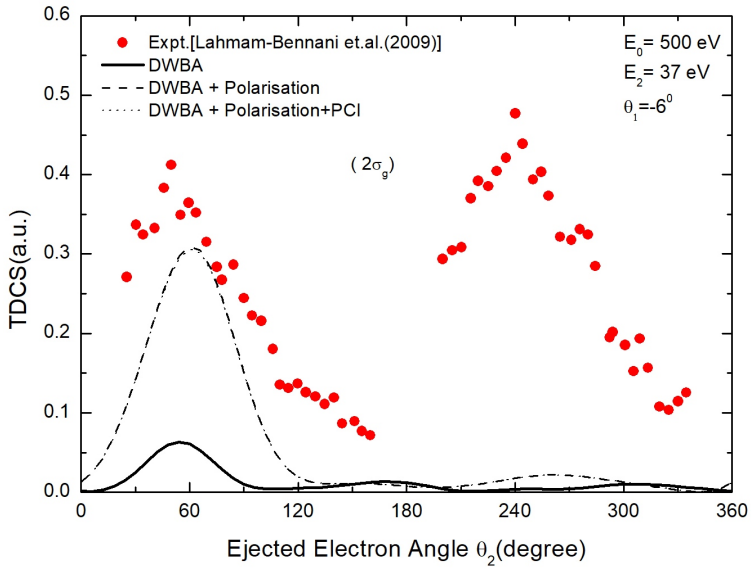


**Figure 7.** TDCS calculation for the ionization of the inner orbital $2\sigma_g$ of $N_2$. The ejected electron energy chosen here is 37 eV. The legends and kinematics are displayed in the Figure frame.

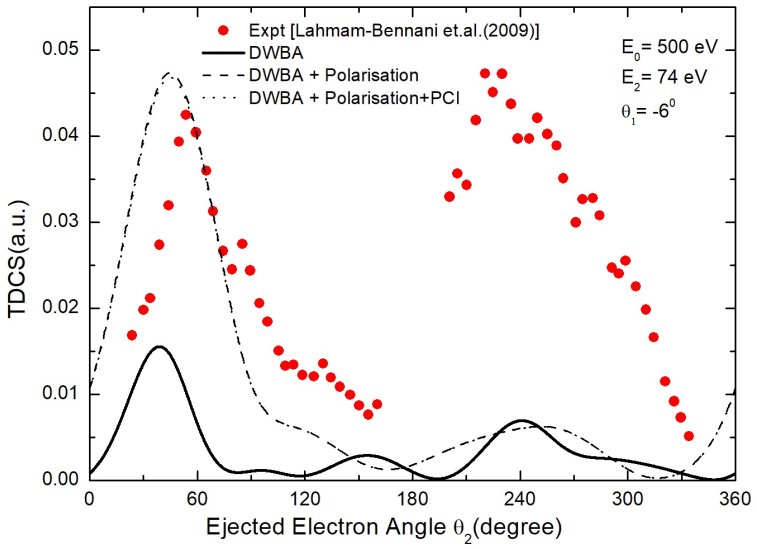


**Figure 8.** Kinematics is same as Figure 4 and the ejected electron energy chosen is 74 eV.

There is a mismatch between theoretical and experimental data in terms of recoil to binary ratio. All theoretical frameworks fail to reproduce the experimental ratio of recoil to the binary peak.

At high ejection energies, better results are reproduced for the recoil region. At 37 eV, no recoil peak can be seen in theoretical results. For 74 eV a small peak is obtained for recoil region, while at 205 eV a better resemblance between the theoretical and experimental results is obtained in the recoil region. Furthermore, the experimental recoil to binary peak ratio is much greater than the theoretical one for all the kinematics chosen. It is believed that the strong interaction between the ejected electron and the residual ion causes a large recoil intensity. This interaction is enhanced for orbitals with an inner valence and targets with multiple electrons and multiple centres [29]. It is clear that the approximation employed in the present study to calculate TDCS requires more efforts to include effects such as multiple scattering, second order effects to analyse available measurements. We have found the inclusion of target polarization potential to be significant up to an extent; however, the PCI is found to be not very significant for the present kinematics.

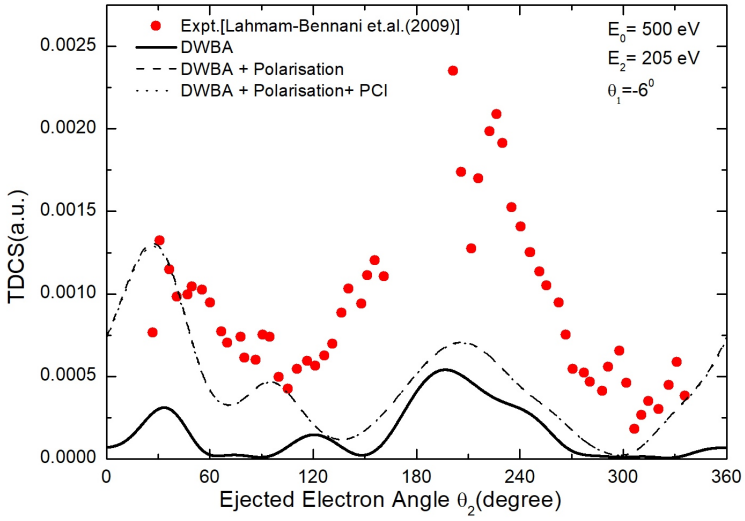


**Figure 9.** Kinematics is same as Figure 4 and the ejected electron energy chosen is 205 eV.

## 4. Conclusions

TDCSs have been calculated for electron impact ionization of outer $3\sigma_g$, $1\pi_u$, $2\sigma_u$ and the 'inner' $2\sigma_g$ molecular orbital of nitrogen molecules. The effect of target polarization and post collision interaction between the scattered and ejected electrons after the collision has also been investigated.

The cross sections have been calculated at 37 eV, 74 eV, and 205 eV ejected energies. Due to the close proximity of the outer orbital, the TDCS results are also presented as the average and weighted sum for these orbital. The TDCS results are analysed in terms of positions and relative magnitudes of binary and recoil peaks. For the outer orbital at 37 eV ejected electron energy, polarization potential has been found significant and the results are in good agreement within the binary region however, PCI is not able to make significant changes in the trends of TDCS. At high ejection energy, the theoretical calculations seem to reproduce better results for the recoil region. There is a high discrepancy at recoil peak for 37 eV but gives a qualitative agreement for 74 eV and 205 eV ejection energy.

In the case of ionization from the inner orbital of the nitrogen molecule, large discrepancies are observed between theoretical and experimental results however polarization potential is found to be significant in the binary peak region. There is a qualitative agreement with the binary peak and poor agreement for the recoil peak. The experimental recoil to binary peak ratio is not well produced by the theoretical methods implied.

The current theory-experiment discrepancies seem to motivate applications of more sophisticated methods for improvement. For instance, it would be worthwhile to examine the trends of TDCS of nitrogen molecules further with the distorted wave second Born approximation.

**Author Contributions:** A.P. and G.P. contributed equally in the writing and analysis of the manuscript. All authors have read and agreed to the published version of the manuscript.

**Funding:** This research was funded by Science and Engineering Research Board (SERB), New 246 Delhi. Grant No. CRG/2019/001059.

**Institutional Review Board Statement:** Not applicable.

**Informed Consent Statement:** Not applicable.

**Data Availability Statement:** The associated data will be available from authors upon request.

**Acknowledgments:** We acknowledge the grant received from Science and Engineering Research Board(SERB), New Delhi in the form of SERB CRG project (CRG/2019/001059).

**Conflicts of Interest:** The authors declare no conflict of interest.

## References


1. Lahmam-Bennani, A. Recent developments and new trends in (e, 2e) and (e, 3e) studies. *J. Phys. B At. Mol. Opt. Phys.* **1991**, *24*, 2401. [CrossRef]
2. Dörner, R.; Mergel, V.; Jagutzki, O.; Spielberger, L.; Ullrich, J.; Moshammer, R.; Schmidt-Böcking, H. Cold target recoil ion momentum spectroscopy: A 'momentum microscope'to view atomic collision dynamics. *Phys. Rep.* **2000**, *330*, 95–192. [CrossRef]
3. Ullrich, J.; Moshammer, R.; Dörner, R.; Jagutzki, O.; Mergel, V.; Schmidt-Böcking, H.; Spielberger, L. Recoil-ion momentum spectroscopy. *J. Phys. B At. Mol. Opt. Phys.* **1997**, *30*, 2917. [CrossRef]
4. Naja, A.; Casagrande, E.S.; Lahmam-Bennani, A.; Stevenson, M.; Lohmann, B.; Dal Cappello, C.; Bartschat, K.; Kheifets, A.; Bray, I.; Fursa, D.V. (e, 2e) triple differential cross-sections for ionization beyond helium: The neon case at large energy transfer. *J. Phys. B At. Mol. Opt. Phys.* **2008**, *41*, 085205. [CrossRef]
5. Lahmam-Bennani, A.; Naja, A.; Casagrande, E.S.; Okumus, N.; Dal Cappello, C.; Charpentier, I.; Houamer, S. Dynamics of electron impact ionization of the outer and inner valence (1t2 and 2a1) molecular orbitals of $CH_4$ at intermediate and large ion recoil momentum. *J. Phys. B At. Mol. Opt. Phys.* **2009**, *42*, 165201. [CrossRef]
6. Mouawad, L.; Hervieux, P.A.; Dal Cappello, C.; El Bitar, Z. Ionization of phenol by single electron impact: Triple differential cross sections. *J. Phys. B At. Mol. Opt. Phys.* **2019**, *53*, 025202. [CrossRef]
7. Singh, P.; Purohit, G.; Champion, C.; Patidar, V. Electron-and positron-induced ionization of water molecules: Theory versus experiment at the triply differential scale. *Phys. Rev. A* **2014**, *89*, 032714. [CrossRef]
8. Wang, Y.; Wang, Z.; Gong, M.; Xu, C.; Chen, X. Theoretical study of (e, 2e) triple differential cross sections of pyrimidine and tetrahydrofurfuryl alcohol molecules using multi-center distorted-wave method. *Chin. Phys. B* **2022**, *31*, 010202. [CrossRef]
9. Al-Hagan, O.; Kaiser, C.; Madison, D.; Murray, A.J. Atomic and molecular signatures for charged-particle ionization. *Nat. Phys.* **2009**, *5*, 59–63. [CrossRef]
10. Pindzola, M.S.; Colgan, J.P.; McLaughlin, B.M. Electron-impact double ionization of the $H_2$ molecule. *J. Phys. B At. Mol. Opt. Phys.* **2018**, *51*, 035206. [CrossRef]
11. Senftleben, A.; Pflüger, T.; Ren, X.; Al-Hagan, O.; Najjari, B.; Madison, D.; Dorn, A.; Ullrich, J. Search for interference effects in electron impact ionization of aligned hydrogen molecules. *J. Phys. B At. Mol. Opt. Phys.* **2010**, *43*, 081002. [CrossRef]
12. Hargreaves, L.R.; Colyer, C.; Stevenson, M.A.; Lohmann, B.; Al-Hagan, O.; Madison, D.H.; Ning, C. (e, 2 e) study of two-center interference effects in the ionization of $N_2$. *Phys. Rev. A* **2009**, *80*, 062704. [CrossRef]
13. Toth, I.; Nagy, L. Ionization of molecular nitrogen by electron impact in (e, 2e) processes. *J. Phys. B At. Mol. Opt. Phys.* **2011**, *44*, 195205. [CrossRef]
14. Murray, A.J.; Hussey, M.J.; Gao, J.; Madison, D. States of $N_2$—comparison between experiment and theoretical predictions of the effects of exchange, polarization and interference. *J. Phys. B At. Mol. Opt. Phys* **2006**, *39*, 3945–3956. [CrossRef]
15. Chaluvadi, H.; Ozer, Z.N.; Dogan, M.; Ning, C.; Colgan, J.; Madison, D. Observation of two-center interference effects for electron impact ionization of $N_2$. *J. Phys. B At. Mol. Opt. Phys.* **2015**, *48*, 155203. [CrossRef]
16. Tachino, CA and Martín, F and Rivarola, RD Theoretical study of interference effects in single electron ionization of N2 molecules by proton impact. *J. Phys. B At. Mol. Opt. Phys.* **2011**, *45*, 025201. [CrossRef]
17. Ozer, Z.N. Differential cross sections of nitrogen containing molecules at intermediate electron impact energy. *AIP Conf. Proc.* **2018**, *2042*, 020027.
18. Morillo-Candas, A.; Silva, T.; Klarenaar, B.; Grofulović, M.; Guerra, V.; Guaitella, O. Electron impact dissociation of $CO_2$. *Plasma Sources Sci. Technol.* **2020**, *29*, 01LT01. [CrossRef]
19. Zhou, J.; Ali, E.; Gong, M.; Jia, S.; Li, Y.; Wang, Y.; Zhang, Z.; Xue, X.; Fursa, D.V.; Bray, I.; et al. Absolute triple differential cross sections for low-energy electron impact ionization of biochemically relevant systems: Water, tetrahydrofuran, and hydrated tetrahydrofuran. *Phys. Rev. A* **2021**, *104*, 012817. [CrossRef]
20. Dhankhar, N.; Choubisa, R. Triple differential cross-section for the twisted electron impact ionization of water molecule. *arXiv* **2021**, arXiv:2108.00692.
21. Fernández-Menchero, L.; Otranto, S. Fully and double differential cross sections for the single ionization of $H_2O$ by bare ion impact. *J. Phys. B At. Mol. Opt. Phys.* **2014**, *47*, 035205. [CrossRef]
22. Mouawad, L.; Hervieux, P.A.; Dal Cappello, C.; Pansane, J.; Robert, V.; El Bitar, Z. Triple differential cross sections for the ionization of pyrimidine by electron impact. *Eur. Phys. J. D* **2019**, *73*, 1–8. [CrossRef]
23. Singh, P.; Champion, C. Theoretical study of (e, 2e) triple-differential cross sections for DNA component ionization by electrons and positrons. *J. Phys. B At. Mol. Opt. Phys.* **2019**, *52*, 075201. [CrossRef]
24. Madison, D.H.; Calhoun, R.V.; Shelton, W.N. Triple-differential cross sections for electron-impact ionization of helium. *Phys. Rev. A* **1977**, *16*, 552. [CrossRef]
25. De Lucio, O.; DuBois, R. Differential studies and projectile charge effects in ionization of molecular nitrogen by positron and electron impact. *Phys. Rev. A* **2016**, *93*, 032710. [CrossRef]
26. Avaldi, L.; Camilloni, R.; Fainelli, E.; Stefani, G. Ionization of the $N_2$ 3 sigma g orbital by electron impact studied by asymmetric (e, 2e) experiments. *J. Phys. B At. Mol. Opt. Phys.* **1992**, *25*, 3551. [CrossRef]
27. Purohit, G.; Kato, D. Projectile charge effects on the differential cross sections for the ionization of molecular nitrogen by positrons and electrons. *J. Phys. B At. Mol. Opt. Phys.* **2018**, *51*, 135202. [CrossRef]

28. Tóth, I.; Campeanu, R.; Chiş, V.; Nagy, L. Electron impact ionization of diatomic molecules. *Eur. Phys. J. D* **2008**, *48*, 351–354. [CrossRef]
29. Lahmam-Bennani, A.; Casagrande, E.S.; Naja, A. Experimental investigation of the triple differential cross section for electron impact ionization of $N_2$ and $CO_2$ molecules at intermediate impact energy and large ion recoil momentum. *J. Phys. B At. Mol. Opt. Phys.* **2009**, *42*, 235205. [CrossRef]
30. Senftleben, A.; Al-Hagan, O.; Pflüger, T.; Ren, X.; Madison, D.; Dorn, A.; Ullrich, J. Fivefold differential cross sections for ground-state ionization of aligned $H_2$ by electron impact. *J. Chem. Phys.* **2010**, *133*, 044302. [CrossRef]
31. Madison, D.H.; Al-Hagan, O. The distorted-wave Born approach for calculating electron-impact ionization of molecules. *J. At. Mol. Phys.* **2010**, *2010*. [CrossRef]
32. Lee, C.; Yang, W.; Parr, R.G. Development of the Colle-Salvetti correlation-energy formula into a functional of the electron density. *Phys. Rev. B* **1988**, *37*, 785. [CrossRef] [PubMed]
33. Furness, J.; McCarthy, I. Semiphenomenological optical model for electron scattering on atoms. *J. Phys. B At. Mol. Phys.* **1973**, *6*, 2280. [CrossRef]
34. Riley, M.E.; Truhlar, D.G. Approximations for the exchange potential in electron scattering. *J. Chem. Phys.* **1975**, *63*, 2182–2191. [CrossRef]
35. Padial, N.; Norcross, D. Parameter-free model of the correlation-polarization potential for electron-molecule collisions. *Phys. Rev. A* **1984**, *29*, 1742. [CrossRef]
36. Ward, S.; Macek, J. Wave functions for continuum states of charged fragments. *Phys. Rev. A* **1994**, *49*, 1049. [CrossRef]